Coherent Electron Acceleration by Subcycle Laser Pulses

Bernhard Rau,[1] T. Tajima,[1] and H. Hojo[2]
[1]*Physics Department, The University of Texas at Austin, Austin, Texas 78712*
[2]*Plasma Research Center, University of Tsukuba, Tsukuba 305, Japan*
(Received 28 June 1996; revised manuscript received 23 December 1996)

Analytic three dimensional solutions for electromagnetic waves correct even for subcyclic pulses have been obtained. It is demonstrated analytically and via $1-2/2$ dimensional PIC (particle in cell) simulations that the irradiation of an intense subcyclic pulse on a thin plasma layer gives rise to a pickup of all plasma electrons on the spot, accelerates them over a small distance, and leads to a short, coherent, and ultracold electron beam. [S0031-9007(97)03038-X]

PACS numbers: 41.75.Lx, 41.20.Jb, 52.40.Nk, 52.75.Di

Ultrafast laser pulse interaction with matter is an important topic of research. The chirped pulse amplification technique [1] has drastically advanced the laser pulse length compression in recent years [2]. Now we witness even generation of subcyclic pulses in the microwave [3], far infrared [4], and femtosecond [5] regimes. We are interested in an intense subcyclic pulse interaction with matter (i.e., plasma, as the pulse is intense). While an intense, short (but not shorter than a single period) pulse injected in an underdense plasma is known to create a wakefield [6], the new physics in this ultrashort (subcyclic) regime beyond the laser wakefield creation is largely unknown. In this Letter, we illuminate some of the issues that arise with this type of interaction. Our work may also be looked upon as a continuation of research for an efficient method to pick up electrons in matter to accelerate to higher energies without severe spread, the so-called problem of injection [7].

Electromagnetic waves (or pulses) shone on a focal region take a three-dimensional expression. Lax *et al.* and other researchers [8,9] have investigated such for a long beam. Here we investigate solutions for a pulse of arbitrary length (and thus inclusive of a subcyclic pulse) propagating in the z direction. Using the vacuum wave equation for the x component of the electric field, we find the closed form expression

$$\tilde{E}_x\left(x,y,z;k=\frac{\omega}{c}\right)=\frac{1}{2\pi}\int dp\int dq A(p,q;k)\times\exp[ik(px+qy+\sqrt{1-p^2-q^2}\,z)] \quad (1)$$

for the Fourier frequency components of E_x. Since we assume the electromagnetic field to be present far away from any sources and boundaries, the limits of integration in Eq. (1) must be chosen in a way that the resulting modes do not exponentially grow or decay, i.e., p, q, and $\sqrt{1-p^2-q^2}$ must be real. Picking $\tilde{E}_x(x,y,z=0;k)=E_0(k)\exp[-r^2/w_0^2]$ and assuming the three-dimensional pulse to have the same frequency spectrum as its one-dimensional counterpart, $A(p,q;k)$ is uniquely determined as $A(p,q;k)=E_0(k)k^2w_0^2/2\exp[-k^2(p^2+q^2)w_0^2/4]$, where $E_0(k)$ is found from the Fourier transform of $E_0\exp[-(z-ct)^2/(2\sigma^2)]\cos[k_0(z-ct)]$ to be $E_0(k)=E_0\sigma\exp[-(k_0^2+k^2)\sigma^2/2]\cosh[kk_0\sigma^2]$. Here, E_0 is the overall amplitude of the laser pulse, w_0 is the spot size of the laser pulse at the focal plane, σ characterizes the pulse length, and k_0 is the k number affiliated with the center frequency of the pulse. With the above choice of $A(p,q;k)$, E_x is cylindrically symmetric in $r=\sqrt{x^2+y^2}$ and the double integral in (1) can be reduced to an integral over the dimensionless variable $b=\sqrt{1-p^2-q^2}$. Inserting $A(p,q;k)$ into (1) and back transforming into time space, we find

$$E_x(r,z,t)=\int_{-\infty}^{\infty}dk\,k^2\int_0^1 db\,F(k,b)\times b\exp[ik(zb-ct)]J_0(kr\sqrt{1-b^2}), \quad (2)$$

with

$$F(k,b)=\frac{E_0w_0^2\sigma}{2\sqrt{2\pi}}\exp\left[-\frac{(k_0^2+k^2)\sigma^2}{2}\right]\cosh[kk_0\sigma^2]\times\exp\left[-\frac{k^2w_0^2(1-b^2)}{4}\right].$$

Assuming further that $E_y(r,z,t)\equiv 0$ for all r, z, and t, the other electromagnetic field components are found using the vacuum Maxwell equations $\vec{\nabla}\cdot\vec{E}=0$ and $\partial\vec{B}/\partial t=-c\vec{\nabla}\times\vec{E}$,

$$E_z(x,y,z,t)=\frac{\partial}{\partial x}\left\{\int_{-\infty}^{\infty}dk\,ik\int_0^1 db\,F(k,b)\times\exp[ik(zb-ct)]J_0(kr\sqrt{1-b^2})\right\}, \quad (3)$$

$$B_x(x,y,z,t)=\frac{\partial^2}{\partial x\,\partial y}\left\{\int_{-\infty}^{\infty}dk\int_0^1 db\,F(k,b)\times\exp[ik(zb-ct)]J_0(kr\sqrt{1-b^2})\right\}, \quad (4)$$

$$B_y(x,y,z,t)=\int_{-\infty}^{\infty}dk\int_0^1 db\,F(k,b)\times\exp[ik(zb-ct)]\left\{k^2b^2-\frac{\partial^2}{\partial x^2}\right\}\times J_0(kr\sqrt{1-b^2}), \quad (5)$$

and

 0031-9007/97/78(17)/3310(4)$10.00 © 1997 The American Physical Society

$$B_z(x,y,z,t) = \frac{\partial}{\partial y}\left\{\int_{-\infty}^{\infty} dk\, ik \int_0^1 db\, F(k,b) \times b \exp[ik(zb - ct)] J_0(kr\sqrt{1-b^2})\right\}. \quad (6)$$

Other authors [9] have argued that the integral over b in Eqs. (2)–(6) can be evaluated to a good approximation as long as $kw_0 > 0.4$ for all frequencies present in the pulse. While this is true for long (monochromatic) pulses, this approximation fails for our cases of short, large bandwidth pulses. In passing, we note that the E_x field (2) can be evaluated in a simpler expression for $r = 0$ and $z = 0$ or z large,

$$E_x(r=0, z=0, t) = E_0 \exp\left[-\frac{c^2t^2}{2\sigma^2}\right]\cos[k_0 ct] - \frac{E_0}{\sqrt{1+\rho^2}} \exp\left[-\frac{k_0^2\sigma^2}{4(1+\rho^2)}\right]\exp\left[-\frac{c^2t^2}{2\sigma^2(1+\rho^2)}\right]\cos\left[\frac{k_0 ct}{1+\rho^2}\right], \quad (7)$$

and

$$E_x\left(r=0, |z|>\sigma; |z|>\frac{w_0^2}{\sigma}, t\right) = \frac{E_0}{2}\exp\left[-\frac{(z-ct)^2}{2\sigma^2}\right] \times \left\{\exp[ik_0(z-ct)]\frac{z - ct - ik_0\sigma^2}{z - ct - ik_0\sigma^2 + z/\rho^2} + \text{c.c.}\right\}, \quad (8)$$

where we defined $\rho = w_0/(\sqrt{2}\,\sigma)$ to be proportional to the ratio of spot size and pulse length. In (7) and (8), E_x approaches the correct limit for a one-dimensional pulse of arbitrary length ($\rho \to \infty$) as well as for a three-dimensional long pulse ($\rho \to 0$ and $\sigma \to \infty$). For $\sigma k_0 \leq \mathcal{O}(1)$, (7) indicates a propagating unipolarlike solution.

On axis, we find $E_z(r=0,z,t) = B_x(r=0,z,t) = B_z(r=0,z,t) = 0$ for all z and t such that we are left with E_x and B_y (Fig. 1) as the only nonvanishing fields. For the fields (2)–(6) inside the focal region ($r \ll w_0$, $|z| \ll w_0$) of a large spot size pulse ($\rho \gg 1$), we can then use the one-dimensional field expressions $E_x = B_y = E_0 \exp[-(z-ct)^2/(2\sigma^2)]\cos[k_0(z-ct)]$ to determine the electron motion due to its interaction with the electromagnetic radiation.

In this regime, we can calculate the single electron motion in an electromagnetic wave traveling in the z direction: The z component of the relativistic Lorentz equation together with the time dependence of the power,

$$\frac{d\,\gamma(1-\beta_z)}{dt} = -e(\vec{\beta}\cdot\vec{E} - E_z - \beta_x B_y + \beta_y B_x) \simeq 0, \quad (9)$$

can be used to find the approximate constant $\gamma(1-\beta_x)$ of the electron motion. Also, for the motion in the y direction, we find

$$m_0 c\,\frac{d(\gamma\beta_y)}{dt} = -e(E_y + \beta_z B_x - \beta_x B_z) \simeq 0. \quad (10)$$

Within this parameter regime, we can follow the analysis of Scheid and Hora [10] to determine the electron motion due to its interaction with a laser pulse of the form (2)–(6) inside the focal region: For $\vec{v}_{\text{init}} = 0$, we integrate the x component of the relativistic Lorentz equation with respect to $u = z - ct$ to obtain $\gamma\beta_x = A \equiv e/(m_0c^2)\int_{-\infty}^{\infty} E_x(u)\,du$, which, with the help of Eq. (9), enables us to write the relativistic Lorentz factor in terms of the initial electric field

$$\gamma_{\text{final}} = 1 + A^2/2.$$

For a wave train with more than a few oscillations, A vanishes in accordance with the Lawson-Woodward theorem [11]. For subcyclic (unipolarlike) pulses, this theorem does not apply and acceleration ($|A| > 0$) takes place.

Introducing the normalized vector potential $a_0 \equiv (eE_0)/(m_0k_0c^2)$, the electron energy gain for an initial wave packet of the form (2)–(6) becomes

$$\Delta E = m_0c^2\pi(k_0\sigma)^2 a_0^2 \exp[-(k_0\sigma)^2]. \quad (11)$$

Maximum gain for a given field amplitude E_0 is thus obtained at $k_0\sigma = 1$, which entails the optimum pulse width being shorter than one wavelength.

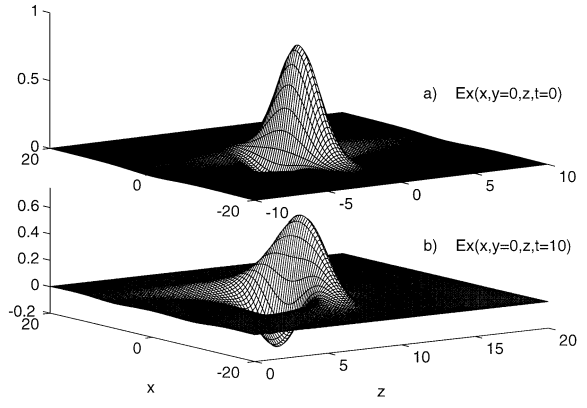

FIG. 1. E_x at (a) $ct = 0$ and (b) $ct = 10\sigma$ for $w_0 = 5\sigma$. The vertical axis is normalized to E_0, and the x and z axes are in units of σ. While the field evolves into a full cycle pulse on axis [see Eq. (8)], the subcyclic character remains visible at the edges. This is due to faster spread of the lower frequency components so that the fields on axis far away from the focal region mainly contain the high frequency components.

In our proposed setup, we inject such an ultrashort laser pulse of high intensity into a plasma slab of finite longitudinal extent. Because of their interaction with the wave packet, the electrons will be expelled from the initial plasma region, while the massive ions remain inertial on such a short time scale. Since an ambipolar electrostatic field E_{amb} will be generated by the separation of plasma electrons and ions, the initial laser pulse must be powerful enough for the electrons to overcome this repulsive force. Using (11), we find the condition $\Delta E > \int_0^\infty E_{\mathrm{amb}}(z)\,dz$, but since $E_{\mathrm{amb}}(z)$ will decay in both the longitudinal direction (due to a finite spot size) as well as in time (due to the response of the remaining plasma outside the transversal focal region), we can estimate the condition to become $m_0c^2\pi(k_0\sigma)^2a_0^2\exp[-(k_0\sigma)^2] > \int_0^{L_p} 4\pi n_0 e^2 z\,dz$, or, assuming $k_0\sigma = 1$,

$$a_0^2 > \frac{\exp(1)}{2\pi}\left(\frac{L_p}{c/\omega_p}\right)^2. \tag{12}$$

Here n_0 is the electron density of the initial plasma, L_p is its longitudinal extent, and ω_p is the plasma frequency. This shows that even small plasma lengths of the order of the plasma skin depth c/ω_p require relativistically strong field amplitudes ($a_0 \geq 1$). Similar to this, we find an upper limit for the number of particles per unit area that can be accelerated per shot,

$$N/S = n_0 L_p < a_0^2/[2r_e L_p \exp(1)], \tag{13}$$

where $r_e = e^2/(m_0c^2)$ and S is the transversal area over which the intensity of the wave packet is nearly constant [typically $\mathcal{O}(1/k_0^2)$]. For plasma lengths of the order of 1 μm, the upper limit for the number of electrons per unit area is $N/S[\mathrm{mm}^{-2}] < a_0^2\mathcal{O}(10^{13})$, which even for moderate values of a_0 seems to be sufficient to fulfill the needs of particles per bunch in modern accelerators/injectors.

In our setup for the 1-2/2 dimensional particle in a cell (PIC) simulations [12], we initialized the pulse in a vacuum region outside the plasma slab and let it evolve into the layer (Fig. 2). After propagation through the finite plasma, the pulse enters the vacuum region behind the slab, carrying with it the expelled electrons. The number of macroparticles used in this simulations was 8000 on a $2^{11}\Delta$ large grid and the plasma was quasineutral. The initial electron distribution was Maxwellian with an electron temperature $T_e = 10$ eV. For the results displayed in Fig. 2, we used a wave packet with $a_0 = 10$, $\omega_0/\omega_p = 30$, and $L_p = 1c/\omega_p$. Since the one-dimensional electrostatic potential created by the charge separation does not decay, we stopped the simulation at a point when the electrons are just about overtaken by the wave packet ($t_{\mathrm{end}} = 15/\omega_p$). In reality, multidimensional effects let the potential decrease at increasing distant (see above). Those effects were manually implemented into our 1-2/2 dimensional PIC code, but since they do not yield any qualitatively different results, we left them out for this Letter.

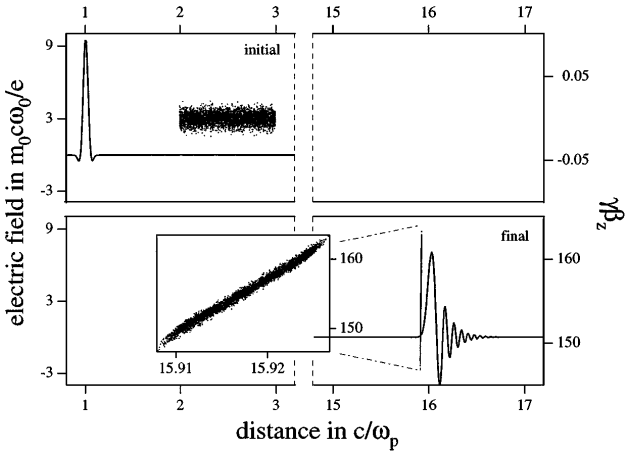

FIG. 2. Initial and final transversal electric field and phase space for $L_p = 1c/\omega_p$, $\omega_0/\omega_p = 30$, and $a_0 = 10$. Inset: blowup of the final longitudinal phase space.

The initial normalized longitudinal emittance is

$$\epsilon_N^{\mathrm{init}} = \sqrt{\frac{1}{12}L_p^2\frac{T_e}{m_0c^2}}\,, \tag{14}$$

or about $4.04 \times 10^{-4}\,L_p[\mu\mathrm{m}]\sqrt{T_e[\mathrm{eV}]}$ mm mrad. Because of the quasi-instantaneous acceleration of the electrons to relativistic velocities, space charge effects are practically absent, so that for strong pulses the longitudinal emittance remains unchanged. In Fig. 3(a) we displayed the phase space volume, an approximant in the adiabatic regime to the emittance ϵ_N, as a function of time for runs with $a_0 = 10$, $\omega_0/\omega_p = 30$, and the 3 different plasma widths $L_p = (1/3,\ 1,\ \text{and}\ 3)c/\omega_p$. The wave packet is initially centered at 1 and the plasma slab starts at $2c/\omega_p$, so that the pulse enters the plasma at a time $t \simeq 1/\omega_p$, causing a big spread in momentum space between the electrons at the left and those at the right edge of the plasma. Once the pulse passes the slab, the spread decreases again and the longitudinal emittance decays to its

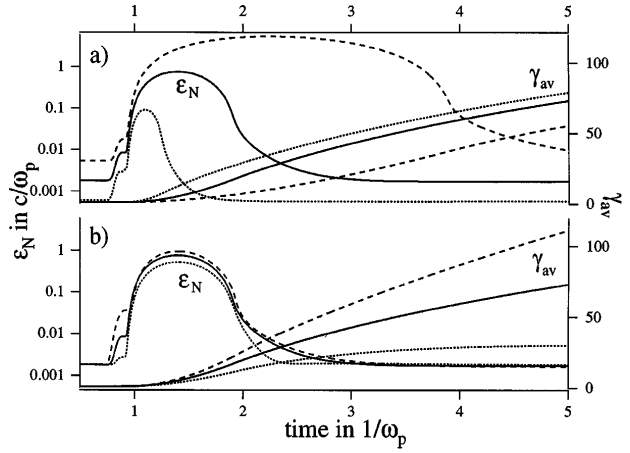

FIG. 3. Normalized phase space volume and γ_{av} as a function of time for (a) $a_0 = 10$, $L_p = \frac{1}{3}$ (dotted), 1 (solid), and 3 (dashed line) c/ω_p and (b) $a_0 = 5$ (dotted), 10 (solid), and 20 (dashed line) $L_p = 1(c/\omega_p)$.

original value, even though the actual distribution becomes stretched along the momentum and compressed along the space axis (see inset of Fig. 2). Figure 3(a) also displays the average relativistic Lorentz factor $\gamma_{\rm av}(t)$ as a function of time for the same three runs. In all three cases, the acceleration of the particles is almost identical as soon as the pulse reached the far end of the plasma slab. In particular, we find the final $\gamma_{\rm av}$ for $L_p = 1$ to be well above 150 (see inset of Fig. 2), compared with the predicted one of $\gamma_{\rm av}^{\rm pred} \simeq 116.6$ [Eq. (11)]. This finds its explanation in the change of group velocity of the laser pulse and hence an increase in interaction time between particles and wave packet. The strong modulation of the final pulse shape (Fig. 2) can be explained by the loss of the pulses dc field component and dispersion effects within the pulse due to the interaction with the electron bunch.

Figure 3(b) shows the average relativistic Lorentz factor $\gamma_{\rm av}$ and the normalized longitudinal emittance ϵ_N for runs with $\omega_0/\omega_p = 30$, $L_p = 1c/\omega_p$, and varied laser intensity $a_0 = 5$, 10, and 20. While ϵ_N returns to its initial value, $\gamma_{\rm av}$ increases with higher a_0. The peak values for $\gamma_{\rm av}$ are found to scale with a_0^2 as expected from Eq. (11), compared to the laser wakefield acceleration with $\gamma_{\rm av} \propto a_0^2\,\omega_0^2/\omega_p^2$ [6,13].

Similar to Eq. (14), the initial normalized transverse emittance is $\epsilon_{N,\rm trans}^{\rm init} = \sqrt{(ST_e)/(\pi m_0 c^2)}$ or about 7.9 $\sqrt{S[\mu{\rm m}^2]T_e[{\rm eV}]}$ mm mrad, where S is the irradiated area of the initial plasma as used in Eq. (13). Because of the three-dimensional nature of the electromagnetic fields, the electron beam might encounter an emittance growth owing to unstable regions of betatron oscillations during the process of acceleration. Additional spread due to the transverse accelerating structure is possible, but those growth rates can be minimized for a geometry with a loose focus [$\rho = w_0/(\sqrt{2}\sigma) \gg 1$].

Here we should point out that the present mechanism does not necessarily require a subcycle pulse. Interaction of electrons and a finite (multicycle) wave train with a sharp rising edge (such that high intensities are reached within the first half-cycle) gives rise to the same acceleration, but requires decoupling of the wave and particles before the electrons enter the second half-cycle.

For the properties stated above (the total electron pickup, ultralow emittance, and energy scaling), the mechanism should work well for a compact particle injector to conventional or novel accelerators as well as a source for high brilliance x rays. In terms of a tabletop electron injector to accelerators, a Ti:sapphire laser ($\lambda_0 \approx 800$ nm) operating at an intensity of 3.6×10^{18} W/cm^2 ($a_0 \simeq 1.3$) and targeted onto a few μm thick plasma layer ($n_e \approx 2 \times 10^{18}/{\rm cm}^3$), we can expect about 3×10^{12} electrons/mm^2 at 1 MeV kinetic energy and with a normalized longitudinal emittance ϵ_N of about 3×10^{-3} mm mrad.

Another future application of this acceleration mechanism might be the use as a bright x-ray source. Because the longitudinal particle bunching is small to begin with [$\mathcal{O}(c/\omega_p)$] and becomes compressed by a factor of about 100 in the process of acceleration (Fig. 2), we may be able to achieve extremely short bunch lengths. Synchrotron radiation becomes coherent (and thus enhanced over the incoherent one by a factor of the number of particles per bunch) if the wavelength λ of the synchrotron radiation is less than the electron bunch length λ_b [14]. With a metallic film [$n_0 = \mathcal{O}(10^{23}/{\rm cm}^3)$] of several ten atomic layers for the initial plasma slab, the electrons can be bunched to only a few Å or less, so that coherent synchrotron radiation in the soft x-ray regime around the "water window" ($\lambda = 2.3$–4.4 nm [15]) can be generated.

Lastly, this mechanism may be also worthy of consideration for eruptive astrophysical acceleration such as γ-ray bursts. Whiplike motion of strong shear-Alfvén waves generated by an instability in an accretion disk or by other phenomena might be able to couple into subcyclic, strong electromagnetic radiation which causes vast acceleration and γ rays.

This work was supported by the U.S. Department of Energy. One of the authors (H. H.) was supported by the Japanese Overseas Research Fellowship.

[1] D. Strickland and G. Mourou, Opt. Commun. **56**, 219 (1985).
[2] C. P. J. Barty *et al.*, Opt. Lett. **21**, 219 (1996).
[3] C. W. Domier *et al.*, Rev. Sci. Instrum. **66**, 339 (1995).
[4] C. Raman, C. W. S. Conover, C. I. Sukenik, and P. H. Bucksbaum, Phys. Rev. Lett. **76**, 2436 (1996).
[5] A. Bonvalet, M. Joffre, J. L. Martin, and A. Migus, Appl. Phys. Lett. **67**, 2907 (1995).
[6] T. Tajima and J. M. Dawson, Phys. Rev. Lett. **43**, 267 (1979).
[7] D. Umstadter, J. K. Kim, and E. Dodd, Phys. Rev. Lett. **76**, 2073 (1996).
[8] M. Lax, W. H. Louisell, and W. B. McKnight, Phys. Rev. A **11**, 1365 (1975); L. W. Davis, Phys. Rev. A **19**, 1177 (1979).
[9] G. P. Agrawal and D. N. Pattanayak, J. Opt. Soc. Am. **69**, 575 (1979); L. Cicchitelli, H. Hora, and R. Postle, Phys. Rev. A **41**, 3727 (1990).
[10] W. Scheid and H. Hora, Laser Part. Beams **7**, 315 (1989).
[11] J. D. Lawson, IEEE Trans. Nucl. Sci. **NS-26**, 4217 (1979); P. M. Woodward, J. IEE **93**, Part III A, 1554 (1947).
[12] T. Tajima, *Computational Plasma Physics* (Addison-Wesley, Reading, MA, 1989); C. K. Birdsall and A. B. Langdon, *Plasma Physics via Computer Simulations* (Adam Hilger, Bristol, England, 1991).
[13] E. Esarey and M. Pilloff, AIP Conf. Proc. **335**, 574 (1995).
[14] J. K. Koga, T. Tajima, and Y. Kishimoto, AIP Conf. Proc. **356**, 424 (1996); T. Nakazato *et al.*, Phys. Rev. Lett. **63**, 1245 (1989).
[15] I. C. E. Turcu *et al.*, J. Appl. Phys. **73**, 8081 (1993); R. A. London, M. D. Rosen, and J. E. Trebes, Appl. Opt. **15**, 3397 (1989).